

## Effect of Charge and Molecular Weight on the Functionality of Gelatin Carriers for Corneal Endothelial Cell Therapy

Jui-Yang Lai,<sup>†,‡</sup> Pei-Lin Lu,<sup>†</sup> Ko-Hua Chen,<sup>‡,§</sup> Yasuhiko Tabata,<sup>||</sup> and Ging-Ho Hsiue<sup>\*,†</sup>

*Department of Chemical Engineering, National Tsing Hua University, Hsinchu, Taiwan 30013, ROC, Division of Medical Engineering, National Health Research Institutes, Taipei, Taiwan 11472, ROC, Department of Ophthalmology, Taipei Veterans General Hospital, Taipei, Taiwan 11217, ROC, and Department of Biomaterials, Institute for Frontier Medical Sciences, Kyoto University, Kyoto 606-8507, Japan*

*Received February 20, 2006; Revised Manuscript Received March 30, 2006*

Cell transplantation strategies usually involve the use of supporting carrier materials because of the soft and fragile nature of these grafts. In this work, a cell-adhesive gelatin hydrogel carrier was fabricated to deliver cultivated human corneal endothelial cell (HCEC) sheets, which were harvested from thermo-responsive poly(*N*-isopropylacrylamide) (PNIPAAm)-grafted culture surfaces. The carrier disks, consisting of gelatins with a different isoelectric point (IEP = 5.0 and 9.0) and a molecular weight (MW) ranging from 3 to 100 kDa, were subjected to 16.6 kGy gamma irradiation for sterilization. The effect of IEP and MW of the raw gelatins (i.e., before irradiation) on the functionality of sterilized disks was studied by determinations of mechanical property, water content, dissolution degree, and cytocompatibility. Irrespective of the IEP of raw gelatin, hydrogel disks prepared with high MW (100 kDa) exhibited a greater tensile strength, lower water content, and slower dissolution rate than those made of low MW gelatin (8 and 3 kDa). From the investigation of cellular responses to the disks, the negatively charged gelatin (IEP = 5.0) groups were more cytocompatible when compared with their positively charged counterparts (IEP = 9.0) at the same MW (100 kDa). Additionally, in the negatively charged gelatin groups, only a slight increase in pro-inflammatory cytokine expression was observed with increasing MW of gelatin from 3 to 100 kDa. It is concluded that the gamma-sterilized hydrogel disks made from raw gelatins (IEP = 5.0, MW = 100 kDa) with appropriate dissolution degree and acceptable cytocompatibility are capable of providing stable mechanical support, making these carriers promising candidates for intraocular delivery of cultivated HCEC sheets.

Functional macromolecules have gained increasing interest because of their potential as stimuli-responsive cell culture substrates<sup>1–3</sup> and supporting cell carriers<sup>4–9</sup> for application in biomedical science. Recently, Okano et al.<sup>10</sup> proposed a novel cell sheet engineering technology for harvesting cultivated cell sheets via temperature modulation of thermo-responsive poly(*N*-isopropylacrylamide) (PNIPAAm)-grafted culture surfaces. The advantage of this method is the possibility of creating transplantable tissue/organ sources without using a three-dimensional biomaterial scaffold, which may elicit host inflammatory responses after in vivo implantation of tissue-engineered replacements into damaged sites.<sup>11</sup> As the thermally detached cell sheets are soft and fragile, the group of Okano also utilized hydrophilically modified poly(vinylidene difluoride) (PVDF) membranes as supporting materials for transportation and surgical handling.<sup>12–14</sup> By employing this scaffold-free tissue engineering technique, various types of well-organized cell sheets have been successfully fabricated to promote tissue regeneration in vivo.<sup>15–18</sup>

Human corneal endothelial cell (HCEC) transplantation aims to restore vision with the hope of reconstituting a structural and functional endothelial monolayer. Therefore, investigators have

attempted to develop tissue equivalents by seeding and cultivating corneal endothelial cells on different carriers made of either natural tissue materials<sup>19,20</sup> or artificial polymeric materials.<sup>4–7</sup> However, intraocular grafting of these tissue-engineered replacements may possibly cause problems such as the unstable attachment of cell carrier membrane to host corneal stroma and fibroblastic overgrowth between the membrane and stroma.<sup>21</sup> By avoiding the permanent residence of foreign carrier materials in the host, our group has recently established a novel strategy based on the concept of cell sheet engineering for corneal endothelial reconstruction.<sup>22</sup> A thermo-responsive PNIPAAm-grafted polyethylene (PE) culture support made by plasma treatment and photografting polymerization was used for the harvest of bioengineered HCEC sheets with proper morphology and function. In addition, we adopted a method to strengthen the transplants by utilizing the transparent and bioadhesive gelatin disks as temporary cell carriers during and after in vivo delivery. This allows the maintenance of tissue-like architecture of implanted cell sheets, which has been proven to be critical to successful graft–host integration and tissue repair.<sup>15</sup>

Gelatin is a naturally occurring biopolymer obtained by the thermal, chemical, or physical denaturation of collagen. It is a biodegradable protein composed of amino acid residues in different proportions and combinations.<sup>23</sup> We have previously shown that the electrical nature of gelatin plays a crucial role in the development of a potential controlled delivery system for bioactive macromolecules such as growth factors,<sup>24,25</sup> protein drugs,<sup>26,27</sup> and plasmid DNAs.<sup>28,29</sup> When electrostatically com-

\* To whom correspondence should be addressed. Phone: +886-3-5719956. Fax: +886-3-5726825. E-mail: ghhsiue@mx.nthu.edu.tw.

<sup>†</sup> National Tsing Hua University.

<sup>‡</sup> National Health Research Institutes.

<sup>§</sup> Taipei Veterans General Hospital.

<sup>||</sup> Kyoto University.

**Table 1.** Physicochemical Characteristics of Raw Gelatins

sample code	collagen source <sup>a</sup>	processing method <sup>a</sup>	isoelectric point <sup>a</sup>	weight-average molecular weight <sup>a</sup> (kDa)	polydispersity index <sup>a</sup>	zeta potential <sup>b</sup> (mV)
G-5-3	bovine bone	alkaline	5.0	3	2.1	-2.3 ± 0.8
G-5-8	bovine bone	alkaline	5.0	8	2.0	-3.1 ± 1.4
G-5-100	bovine bone	alkaline	5.0	100	2.3	-8.2 ± 2.7
G-9-100	porcine skin	acidic	9.0	100	2.5	8.5 ± 2.1

<sup>a</sup> Supplier data. <sup>b</sup> Measured by Doppler microelectrophoresis. Data are expressed as mean ± standard error of the mean (*n* = 5).

plexed with a positively or negatively charged gelatin, a bioactive substance with an opposite charge can be modified to increase its stability, targeting, and sustained release, leading to enhanced therapeutic efficacy. On the other hand, by using a thermo-conductive trephine device, we have prepared the deformable sandwich-like gelatin membranes for encapsulation and transplantation of intact fetal retinal sheets.<sup>30</sup> Because of its hydrogel property, gelatin is also beneficial for a wide range of tissue engineering applications by providing a temporary and hydrated support structure during tissue reconstruction.<sup>31-33</sup>

Gelatin has been recognized as an inert biomaterial,<sup>34-37</sup> and its physicochemical properties such as isoelectric point (IEP) and molecular weight (MW) can be readily modulated by the processing method of collagen.<sup>38</sup> It is known that the charge and the degree of polymerization of macromolecules may affect their cell affinity. Choksakulnimitr et al.<sup>39</sup> reported that a variety of polycations including protamine, poly(L-lysine), and histone induced cellular damage in cultured cells, whereas neutral polymers or polyanions showed no cytotoxicity. Moreover, poly(L-lysine) with high MW was more cytotoxic than those with low MW. In the present paper, a biodegradable and cell-adhesive gelatin carrier was developed for intraocular delivery of the thermally detached HCEC sheets with uniform cell polarity. The mechanical strength, water content, dissolution degree, and cytocompatibility of gamma-sterilized hydrogel disks prepared with raw gelatins (i.e., before irradiation) of different IEPs and MWs were investigated to give insight into the effect of charge and degree of polymerization on the functionality for biomacromolecular carriers. Additionally, we performed an *in vivo* study in a rabbit model to examine the efficacy of the use of gelatin hydrogels as HCEC sheet carriers for enhancing the graft-host integration.

## Experimental Section

**Materials.** Gelatins, prepared through an alkaline processing of bovine bone collagen or an acidic processing of porcine skin collagen, were kindly supplied by Nitta Gelatin (Osaka, Japan). According to information from the supplier, the gelatin samples used as raw materials had IEPs of 5.0 and 9.0, and a weight-average MW range of 3–100 kDa, as well as a polydispersity index of 2.0–2.5 (Table 1). In this study, a gelatin sample with an IEP of 5.0 and a weight-average MW of 3 kDa was designated as G-5-3. The zeta potential of each gelatin was quantified using Doppler microelectrophoresis (Zetasizer 3000HS, Malvern Instruments, Worcestershire, U.K.) and was determined from five independent measurements. Table 1 shows that, although the zeta potential of gelatin samples G-9-100 was positive (8.5 ± 2.1 mV), the zeta potential of gelatin samples G-5-100 was negative (-8.2 ± 2.7 mV). In a series of negatively charged gelatin samples G-5-3, G-5-8, and G-5-100, the zeta potential decreased as the MW decreased. Balanced salt solution (BSS, pH 7.4) was purchased from Alcon Laboratories (Fort Worth, TX). OPTI-modified Eagle's medium (OPTI-MEM), gentamicin, and trypsin-EDTA were purchased from Gibco BRL (Grand Island, NY). Fetal bovine serum (FBS) and the

antibiotic/antimycotic (A/A) solution (10 000 U/mL of penicillin, 10 mg/mL of streptomycin, and 25 µg/mL of amphotericin B) were obtained from Biological Industries (Kibbutz Beit Haemek, Israel). All of the other chemicals were of reagent grade and used as received.

**Preparation of Gelatin Hydrogel Disks.** The gelatin hydrogel disks were prepared by solution casting methods as described elsewhere.<sup>30</sup> Briefly, an aqueous solution of 10 wt % gelatin (40 mL) was cast into a polystyrene planar mold (5 × 5 cm<sup>2</sup>, 1.5 cm depth) and air-dried for 3 days at 25 °C to obtain hydrogel sheets. Using a 7-mm diameter corneal trephine device, the hydrogel sheets were cut out to create small gelatin disks (0.4 cm<sup>2</sup>, 700–800 µm thick). Prior to following tests, the gelatin hydrogel sheets and disks were sterilized by gamma irradiation using a cobalt-60 source located at the National Tsing Hua University (Hsinchu, Taiwan, ROC). According to our earlier report,<sup>30</sup> irradiation was performed in the presence of air at a dose of 16.6 kGy, applied at a dose rate of 0.692 kGy/h; irradiation temperature, 25 ± 1 °C.

**Tensile Tests.** The mechanical properties of the gelatin carriers were measured with an Instron Mini 44 universal testing machine (Canton, MA). Dumbbell-shaped specimens were cut from gelatin hydrogel sheets using a punch. The gauge length of the specimens was 10 mm, and the width was 5 mm. The thickness of each sample was measured at three different points with a Pocket Leptoskop electronic thickness gauge (Karl Deutsch, Germany), and the average was taken. Experiments were run out at 25 °C and relative humidity of 50% using a crosshead speed of 0.5 mm/min. Results were averaged on twelve independent measurements.

**Determination of Water Content and Dissolution Degree.** To measure the water content and dissolution degree of the gelatin disks, the samples were first dried to constant weight (*W<sub>i</sub>*) in vacuo and were immersed in BSS at 34 °C (physiological temperature of the cornea) with reciprocal shaking (125 rpm) in a thermostatically controlled water bath. The swollen hydrogel disks were withdrawn on a filter paper at certain time intervals during the short-term incubation, i.e., within 1 day. After removal of excess superficial water, the weight of disk samples at the swollen state (*W<sub>s</sub>*) was assessed, and the water content was defined by  $((W_s - W_i)/W_s) \times 100$  as described previously.<sup>28</sup> The gross appearances of swollen hydrogel disks were also photographed by a digital camera (Nikon, Melville, NY). After a long-term incubation (1 day to 2 months), the gelatin disks were dissolved and dried in vacuo again. The dry weight of disk samples after dissolution (*W<sub>d</sub>*) was determined and the dissolution degree was calculated as  $((W_i - W_d)/W_i) \times 100$ . All experiments were conducted in triplicate.

**Cell Culture.** This research followed the tenets of the Declaration of Helsinki involving human subjects and was approved by Institutional Review Committee of Taipei Veterans General Hospital. Twenty-eight corneas from human donors (age >50 years) stored in Optisol-GS (Bausch & Lomb, Rochester, NY) at 4 °C were obtained from National Disease Research Interchange (Philadelphia, PA). Primary culture of adult HCECs was performed in accordance with the protocols established previously.<sup>40</sup> After dissociation and collection, the harvested cells were maintained in regular growth medium containing OPTI-MEM as a basal medium, 15% FBS, 50 µg/mL of gentamicin, 1% A/A solution, and other supplements as reported earlier.<sup>40</sup> Cultures were incubated in a humidified atmosphere of 5% CO<sub>2</sub> at 37 °C. The medium was changed every other day. After 1 week in culture, confluent cell

monolayers were subcultured by treating with trypsin-EDTA for 2 min and seeded at a 1:3 split ratio. HCECs were used between passage 2 and 4 during all experiments.

**Cell Proliferation Assay.** For evaluation of cell growth, a modified testing protocol was used as described elsewhere.<sup>41</sup> HCECs ( $7 \times 10^4$  cells/well) were seeded in 24-well plates containing regular growth medium and incubated overnight to allow cells to attach. Cells were then synchronized in the G0-phase of the cell cycle (quiescence) by a further incubation for 24 h in medium containing 0.5% FBS. After synchronization, the medium was replaced with fresh OPTI-MEM containing 2% FBS, to mimic the lower serum conditions of the anterior chamber in vivo.<sup>42</sup> Using cell culture inserts (Falcon 3095, Becton Dickinson Labware, Franklin Lakes, NJ), each well of a 24-well plate was divided into two compartments. A disk sample was placed into the inner well of the double-chamber system to examine the cultures after exposure to gelatin hydrogels. HCECs in OPTI-MEM containing 2% FBS without gelatins served as control groups.

After 48 h of incubation, the cells from each culture well were presumed to have completed their first cell cycle, and the qualitative and quantitative assays were performed following removal of the inserts and gelatins. Cell morphology was observed by phase-contrast microscopy (Nikon). Furthermore, cell growth was estimated using the CellTiter 96 Aqueous Non-Radioactive Cell Proliferation MTS Assay (Promega, Madison, WI), in which the MTS tetrazolium compound is bio-reduced by cells to form a water-soluble colored formazan. The amount of colored product is proportional to the number of metabolically active cells. 100  $\mu$ L of the combined MTS/PMS (20:1) reagent was added to each well of the 24-well plate, and incubated for 3 h at 37 °C in a CO<sub>2</sub> incubator. The data of absorbance readings at 490 nm were measured using the Multiskan Spectrum Microplate Spectrophotometer (ThermoLabsystems, Vantaa, Finland). All experiments were performed in quadruplicate, and the results were expressed as relative MTS activity when compared to control groups.

**Cell Viability Assay.** HCECs were plated on PNIPAAm-grafted PE culture dishes at a density of  $4 \times 10^4$  cells/cm<sup>2</sup> and maintained in regular growth medium at 37 °C. After 3 weeks of cultivation, a gelatin disk was placed on the apical cell surface in direct contact with the confluent monolayers and further incubated for 48 h. Confluent cultures without contacting disk samples served as control groups. Cell viability was determined using a membrane integrity assay, the Live/Dead Viability/Cytotoxicity Kit (Molecular Probes, Eugene, OR) which contains calcein AM and ethidium homodimer-1 (EthD-1). It depends on the intracellular esterase activity to identify the living cells, which cleaves the calcein AM to produce a green fluorescence. In dead cells, EthD-1 can easily pass through the damaged cell membranes to bind to the nucleic acids, yielding a red fluorescence. After washing three times with phosphate-buffered saline (PBS, pH 7.4) to remove undissolved gelatin residue, the monolayered cultures were detached as a cell sheet at 20 °C and stained with a working solution consisting of 2  $\mu$ L of EthD-1, 1 mL of PBS, and 0.5  $\mu$ L of calcein AM. Under fluorescence microscopy (Nikon), three different areas each containing approximately 500 cells were counted at 100 $\times$  magnification. All experiments were performed in duplicate, and the viability of the HCEC sheets was expressed as the average ratio of live cells to the total number of cells in these six different areas.

**Cytokine Expression.** HCECs were grown to confluence on 24-well plates in regular growth medium. When the cells appeared confluent, the medium was replaced with fresh OPTI-MEM containing 2% FBS and a completely dissolved gelatin disk. After incubation at 37 °C for 2 days, the release of interleukin-6 (IL-6) from cultivated cells into the conditioned medium was detected by the Quantikine enzyme-linked immunosorbent assay (ELISA) kit (R&D Systems, Minneapolis, MN) specific for human IL-6. Aliquots of the supernatant collected from the cultures in absence of gelatins served as control groups. Cytokine bioassays were performed according to the manufacturer's instructions. Photometric readings at 450 nm were measured

using the Spectrophotometer (ThermoLabsystems). Results were expressed as pg/mL. All experiments were conducted in quadruplicate.

**Gelatin Carriers for Cell Sheet Delivery.** Preparation of transplantable HCEC sheets on thermo-responsive PNIPAAm-grafted PE surfaces has been described elsewhere.<sup>22</sup> After surface sterilization with ultraviolet light for 2 h in the laminar flow hood,<sup>43</sup> HCECs ( $4 \times 10^5$ ) were seeded in 35-mm diameter PNIPAAm-grafted culture dishes and incubated under the same conditions as mentioned for primary cell culture. After a 3-week cultivation period, the thermo-responsive culture dishes containing confluent cultures were rinsed twice with warmed PBS and replenished with serum-free OPTI-MEM. For the harvest of HCEC sheets, the culture temperature was changed from 37 to 20 °C. Cell monolayers were detached from PNIPAAm-grafted surfaces after incubation at 20 °C for 45 min. Then, the gamma-sterilized hydrogel disks made from raw gelatins (IEP = 5.0, MW = 100 kDa) were immediately placed on apical surface of HCEC sheets to create the gelatin-HCEC sheet constructs for in vivo transplantation studies.

Four adult New Zealand white rabbits (National Laboratory Animal Breeding and Research Center, Taipei, Taiwan, ROC) weighing 3.0–3.5 kg with clinically normal eyes were used in the experiment and treated in accordance with the ARVO Statement for the Use of Animals in Ophthalmic and Vision Research. Animal experiments were carried out at the Institute of Experimental Animal Science, Taipei Veterans General Hospital (Taipei, Taiwan, ROC). As previously described, rabbit corneal endothelium was treated with 0.1 mg/mL of mitomycin-C (Sigma-Aldrich, St. Louis, MO) for 2 weeks to establish an animal model mimicking human corneas.<sup>22</sup> For HCEC sheet transplantation, the rabbits were anesthetized intramuscularly with 10 mg/kg body weight of xylazine hydrochloride (Chanelle, Loughrea, Co. Galway, Ireland) and 60 mg/kg body weight of ketamine hydrochloride (Merial, Lyon, France), and topically with two drops of 0.5% proparacaine hydrochloride (Alcon-Couvreur, Puurs, Belgium). After disinfection and sterile draping of the operation site, the pupil was dilated with one drop of 1% atropine sulfate (Oasis, Taipei, Taiwan, ROC), and a lid speculum was placed. In the right eye of each rabbit, the cornea was penetrated near the limbus with a slit knife under the surgical microscope (Carl Zeiss, Oberkochen, Germany). The central 7 mm of corneal endothelium was removed using a silicone-tipped cannula. Subsequently, the sclerocorneal incision was enlarged to 7.5 mm with scissors, and the gelatin-HCEC sheet constructs were implanted into the anterior chamber. The incision site was closed with three interrupted 10–0 nylon sutures. After surgery, 1% chlortetracycline hydrochloride ophthalmic ointment (Union, Taipei, Taiwan, ROC) was immediately applied to the ocular surface. For topical administration of corticosteroids, each rabbit eye received two drops of 0.3% gentamicin sulfate (Oasis, Taipei, Taiwan, ROC) and one drop of 1% prednisolone acetate (Allergan, Westport, Co. Mayo, Ireland) four times a day during the follow-up period of 6 weeks. Animals were observed by slit-lamp biomicroscopy (Topcon Optical, Tokyo, Japan).

**Statistical Analysis.** All experimental results were expressed as mean  $\pm$  standard error of the mean. Comparative studies of means were analyzed using Student's *t*-test (two-tailed) with a statistical significance at  $p < 0.05$ .

## Results and Discussion

**Tensile Tests.** The stress at break, the strain at break, and the Young's modulus of various gelatin hydrogel carriers are listed in Table 2. In the case of raw gelatins with low MW, no significant difference was observed in the tensile properties between G-5–3 and G-5–8 groups ( $p > 0.05$ ). In contrast, the test specimens from G-5–100 and G-9–100 groups exhibited the stress at break of  $13.1 \pm 3.2$  and  $11.8 \pm 3.5$  MPa, strain at break of  $162 \pm 30$  and  $181 \pm 32\%$ , and Young's modulus of  $69.8 \pm 6.1$  and  $57.5 \pm 9.3$  MPa, respectively. The values of these tensile results were significantly higher than those obtained for the G-5–3 and G-5–8 groups ( $p < 0.05$ ). Recently, the



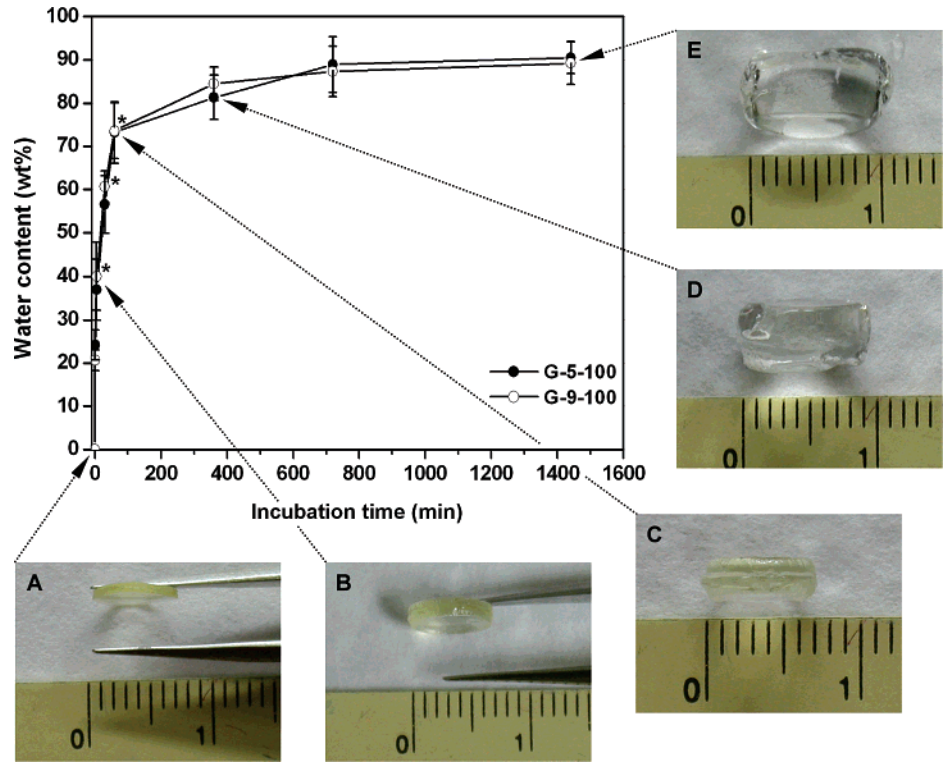


**Figure 1.** Time course of water content of various gelatin hydrogel disks after incubation in BSS at 34 °C. An asterisk indicates statistically significant differences (\**p* < 0.05; *n* = 3) for the mean value of water content compared to value at previous time point. Typical gross photographs of gelatin disks (MW = 100 kDa) are shown (A) before testing and after incubation for distinct time periods (B) 5, (C) 60, (D) 360, and (E) 1440 min. Scale bars from “0” to “1” represent 1 cm.

**Table 2.** Tensile Properties of the Gelatin Hydrogel Carriers<sup>a</sup>

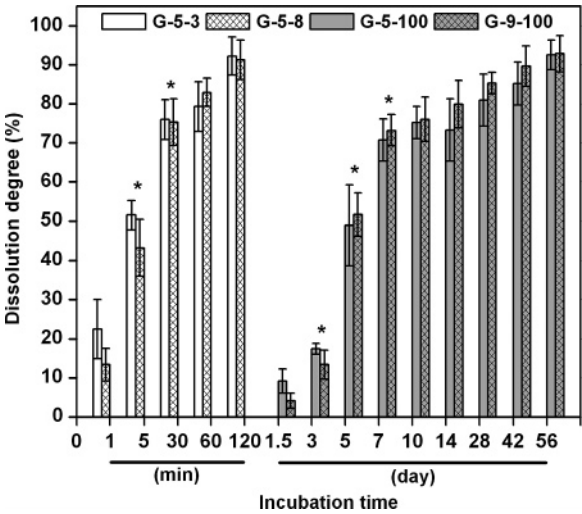
sample code	stress at break (MPa)	strain at break (%)	Young's modulus (MPa)
G-5-3	4.6 ± 1.4	113 ± 28	30.7 ± 3.4
G-5-8	5.4 ± 1.7	109 ± 17	35.4 ± 2.9
G-5-100	13.1 ± 3.2 <sup>b</sup>	162 ± 30 <sup>b</sup>	69.8 ± 6.1 <sup>b</sup>
G-9-100	11.8 ± 3.5 <sup>b</sup>	181 ± 32 <sup>b</sup>	57.5 ± 9.3 <sup>b</sup>

<sup>a</sup> Data are expressed as mean ± standard error of the mean (*n* = 12).  
<sup>b</sup> Significant difference as compared to the G-5-3 groups (*p* < 0.05).

variations of the Bloom number, an index that is proportional to the MW of gelatin, have been shown to affect the mechanical properties of the gelatin films.<sup>44</sup> Due to the increase of triple-helix content, gelatin samples having higher Bloom index displayed greater tensile strength and extensibility. Our data were compatible with these previous results and implied the gamma-sterilized hydrogel carriers made from high MW gelatin (100 kDa) can provide stable mechanical support for thermally detached HCEC sheets.

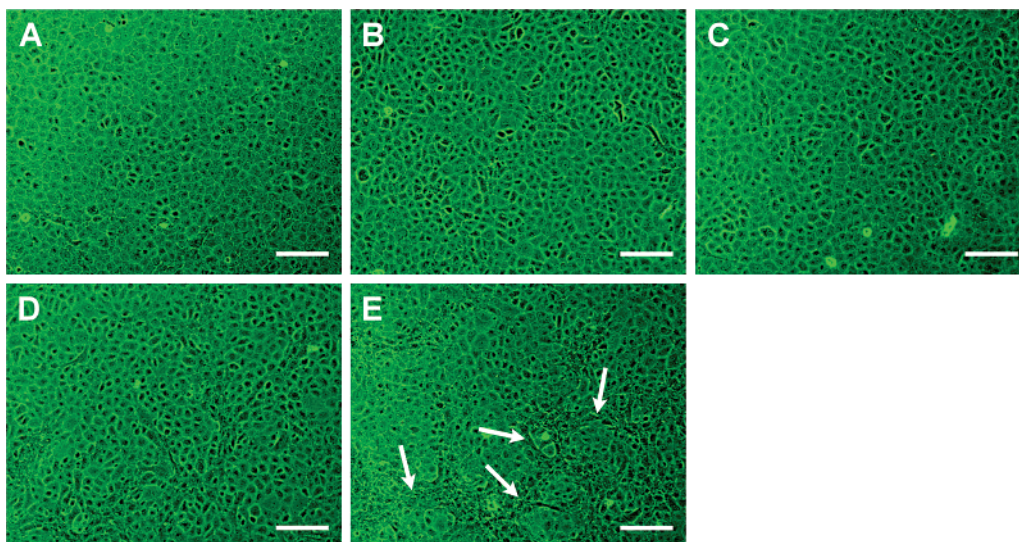
**Determination of Water Content and Dissolution Degree.**

Figure 1 shows water content measurements of different types of gelatin hydrogel disks. In this study, water content is represented by the gain in weight of a dried material after incubation in physiological medium (BSS) at 34 °C. At each time point, the measured water content of gelatin disks did not show any significant difference between the G-5-100 and G-9-100 groups (*p* > 0.05). This result indicated that the IEP of raw gelatin gives no influence on the water content of gamma-sterilized hydrogel carriers. It has been previously reported that the mechanism of hydration of gelatin is a capillary phenomenon of water molecules penetrating the tiny interstices of a collagen-like four-dimensional structure in the gelatin.<sup>45</sup> In this study, the rapid hydration and complete dissolution of the hydrogel disks made of low MW gelatin (3 kDa and 8 kDa) occurred



**Figure 2.** Time course of dissolution degree of various gelatin hydrogel disks after incubation in BSS at 34 °C. An asterisk indicates statistically significant differences (\**p* < 0.05; *n* = 3) for the mean value of dissolution degree compared to value at previous time point.

after a few minutes of incubation in BSS (data not shown). In the G-5-100 and G-9-100 groups, the water contents of disk samples increased rapidly with incubation time up to 60 min and leveled off thereafter. As shown in Figure 1A, the dried hydrogel disks prepared with raw gelatin of high MW (100 kDa) appeared as a rigid disk initially. During a 1440-min incubation in BSS, these disk samples became swollen and transparent (Figure 1B–E). Additionally, water content measurements showed a 2-fold (5 min), 4-fold (60 min), 7-fold (360 min), and 10-fold (1440 min) increase in the weight of swollen hydrogel disks that were significantly higher compared to the dried samples.



**Figure 3.** Phase-contrast micrographs of HCEC cultures. The pattern of cell growth in (A) controls (without materials) after a 2-day exposure to different types of gelatin disks (B) G-5-3, (C) G-5-8, (D) G-5-100, and (E) G-9-100. Malformed cell clusters (arrows) are presented in (E). Scale bars: 100  $\mu\text{m}$ .

The *in vitro* dissolution testing of various gelatin hydrogel disks was performed in BSS at 34 °C (Figure 2). In this study, dissolution degree is represented by the loss in weight of a dried material. For each time point, no significant difference was observed in the dissolution degree between G-5-3 and G-5-8 groups and between G-5-100 and G-9-100 groups ( $p > 0.05$ ). The hydrogel disks prepared with low MW gelatin (3 and 8 kDa) were dissolved for a shorter time period, whereas the time period of disk dissolution became longer with an increase in the MW of raw gelatin. These findings indicated that the *in vitro* dissolution rates of gamma-sterilized hydrogel carriers depended heavily on the MW of raw gelatin. In the G-5-3 and G-5-8 groups, the dissolution degree reached a plateau level of approximately 76% within 30 min. These gelatin disks dissolved in physiological solution too fast to be used for cell sheet delivery. In the case of G-5-100 and G-9-100 groups, the dissolution degree had increased by 7 days and continued to increase by about 92% at 56 days. This result suggested that the implanted hydrogel carriers made of high MW gelatin (100 kDa) in the anterior chamber can be dissolved to an extent required for the establishment of close contact between the graft and defective tissues.

**Cell Proliferation Assay.** Cell-material interaction is of great importance in the evaluation of the biomaterial compatibility. Thus, we began a preliminary investigation of cellular responses to various gelatin hydrogel disks using an indirect contact methodology reported by Trudel et al., who were examining the cytocompatibility of polysaccharide-based hydrogels to vascular smooth muscle cells.<sup>46</sup> As shown in Figure 3A, when the HCECs reach confluence, the cultures in the control groups grow as a contact-inhibited monolayer and can be easily identified by cellular hexagonality. It has been reported that cellular hexagonality is a sensitive indicator of endothelial damage or instability and may be valuable in qualitative observations of cell appearance.<sup>47</sup> After a 2-day exposure to the hydrogel disks made of negatively charged gelatin samples G-5-3, G-5-8, and G-5-100, cells remain healthy and cannot be distinguished from the control groups (Figure 3B–D). However, the morphology of cells exposed to the disks prepared with positively charged gelatin sample G-9-100 is changed (Figure 3E). It was noteworthy that the malformed cells exhibited a tendency to form rosette-like clusters, which were

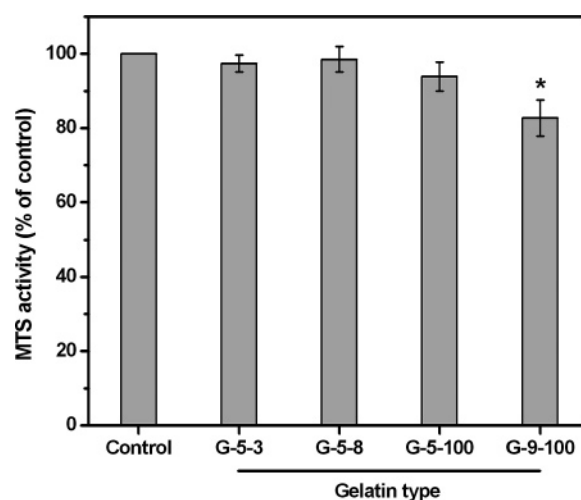


**Figure 4.** Cell proliferation assay of HCEC cultures incubated for 2 days at 37 °C with various gelatin hydrogel disks. Results are expressed as percentage of controls (MTS activity of cells cultured in the absence of materials). An asterisk indicates statistically significant differences ( $*p < 0.05$ ;  $n = 4$ ) as compared to controls.

found in neuroretinal cell cultures for biocompatibility assessment of ophthalmic biomaterials.<sup>48</sup> The cytopathogenesis of rosette formation is not well understood, but it is thought to be a general injury response to foreign stimuli. One possible explanation for these observations is that the corneal endothelial cells are derived from the neural crest during development and are highly sensitive to dissolution products from the hydrogel disks made of positively charged gelatin samples.

Quantitative analysis for HCEC growth was performed following the cell proliferation MTS assay, and the results are also shown in Figure 4. Through the evaluation of mitochondrial dehydrogenase activity (MTS activity), the cell growth did not show a significant difference between the control, G-5-3, G-5-8, and G-5-100 groups ( $p > 0.05$ ) after 2 days in culture. In contrast, the MTS activity was significantly reduced by about 17% ( $p < 0.05$ ) for G-9-100 as compared to those of the control groups. Additionally, cells exposed to hydrogel disks made of gelatin sample G-9-100 were less metabolically active than those from the G-5-100 group ( $p < 0.05$ ). These results clearly



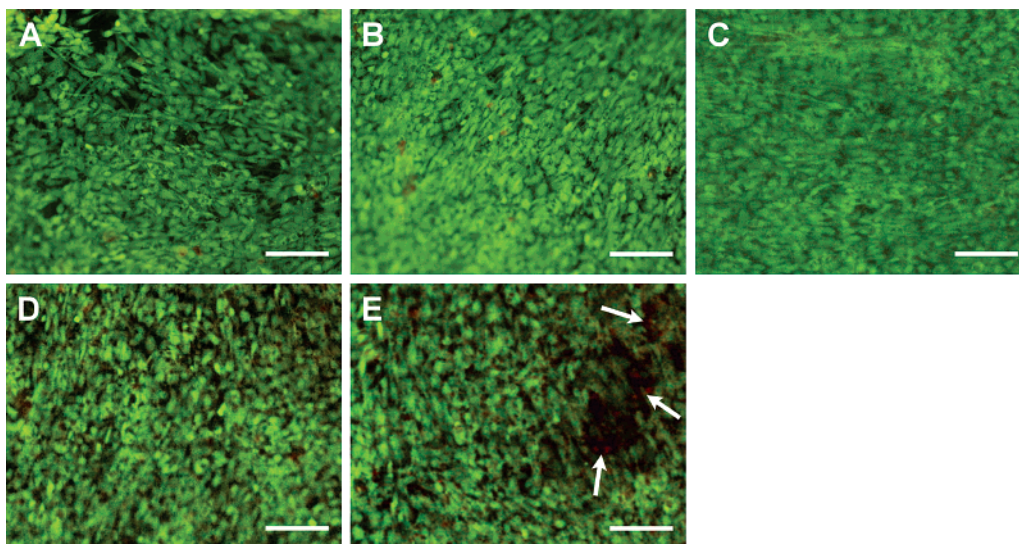


**Figure 5.** Live/Dead assay of the thermally detached HCEC sheets. Fluorescent images of cells in (A) controls (without materials) after direct contact with different types of gelatin disks (B) G-5-3, (C) G-5-8, (D) G-5-100, and (E) G-9-100 for 2 days at 37 °C. Cells were double-stained to be green for live cells and red for dead cells. In panel E, the dead cells are arranged in a rosette-like formation (arrows). Scale bars: 100  $\mu$ m.

demonstrate that the charge of raw gelatin is a potential factor involved in the regulation of corneal endothelial cell proliferation.

**Cell Viability Assay.** Viability tests for the HCEC sheets were carried out in order to further compare the effects of IEP and MW of raw gelatins. Figure 5 is a representative photograph of HCECs labeled with Live/Dead stain, where the live cells fluoresce green and the dead cells fluoresce red. In the control groups, the majority of confluent HCEC monolayers remain viable after detachment at 20 °C (Figure 5A). This finding suggested that the low-temperature incubation did not compromise cell viability. After direct contact with the hydrogel disks made of negatively charged gelatin samples G-5-3, G-5-8, and G-5-100 for 2 days at 37 °C, the HCEC sheets maintain good cell viability with only a few dead cells (Figure 5B–D). However, an increased number of red-stained nuclei were seen in cells exposed to the disks prepared with positively charged gelatin sample G-9-100 (Figure 5E). We also noted that these dead cells displayed a similar pattern of rosette-like formation, as indicated by cell proliferation assay. Figure 6 shows the mean percentage of live cells as determined by the Live/Dead assay. In comparison with control groups, the hydrogel disks consisting of negatively charged gelatins (IEP = 5.0) did not induce any significant changes in cell viability of HCEC sheets, irrespective of the MW of raw gelatin ( $p > 0.05$ ). After a 2-day incubation with the disks made from positively charged gelatins (IEP = 9.0), cell viability was significantly reduced to  $90.3 \pm 2.9\%$  ( $p < 0.05$ ). For the delivery of thermally detached HCEC sheets, these results suggested that the gamma-sterilized hydrogel carriers made from gelatin with negative charge were more cytocompatible than those with positive charge.

**Cytokine Expression.** IL-6 is expressed by a number of cell types and has a crucial role in host defense and immune responses. Due to the increased HLA class II antigen expression, this cytokine is considered to be involved in corneal grafting.<sup>49</sup> After 2 days in culture, the HCEC secretion of IL-6 in response to different types of gelatin hydrogel disks is shown in Figure 7. The expression of IL-6 in the control, G-5-3, G-5-8, G-5-100, and G-9-100 groups was  $116.7 \pm 21.4$ ,  $123.1 \pm 15.4$ ,  $136.2 \pm 24.3$ ,  $180.4 \pm 35.2$ , and  $245.9 \pm 19.8$  pg/mL, respectively. The exposure of HCECs to the disks prepared with negatively charged gelatins (IEP = 5.0) of higher MW induced

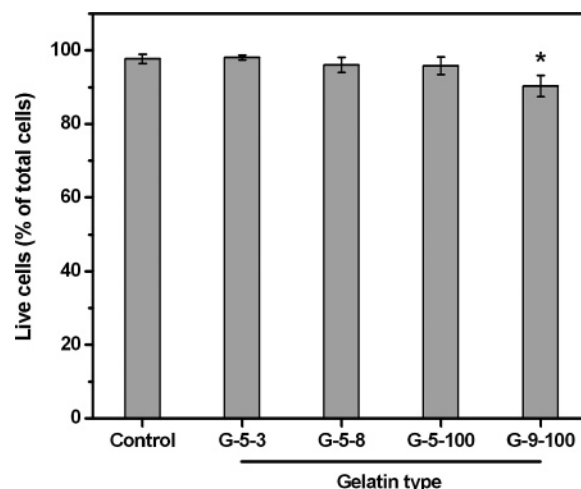


**Figure 6.** Mean percentage of live cells in the HCEC sheets incubated in direct contact with various gelatin hydrogel disks as determined by the Live/Dead assay. An asterisk indicates statistically significant differences ( $p < 0.05$ ;  $n = 6$ ) as compared to controls (without materials).

higher levels of IL-6, although these differences were not significant ( $p > 0.05$ ). The levels of IL-6 were significantly elevated in the medium of G-9-100 groups, compared with those of the control and G-5-100 groups ( $p < 0.05$ ). These results clearly demonstrate that the charge and the degree of polymerization of raw gelatin have an important influence on the stimulation of pro-inflammatory cytokine IL-6 production in HCECs.

**Gelatin Carriers for Cell Sheet Delivery.** Despite having a tissue-like architecture, the thermally detached cell sheets were easily wrinkled and folded during removal of the thermo-responsive culture substrates.<sup>12,13</sup> In the field of cell sheet transfer, Okano et al. have introduced PVDF membranes as a supporter, which renders for the three-dimensional manipulation of cardiomyocyte sheets into layered constructs.<sup>13,15</sup> Moreover, using a doughnut-shaped PVDF supporter, recent attempts have been made to reconstruct ocular surface by transplantation of cultured epithelial cell sheets originating from autologous corneas<sup>14</sup> or oral mucosas.<sup>16</sup> The results of these works have been encouraging since the visual acuity of patients who

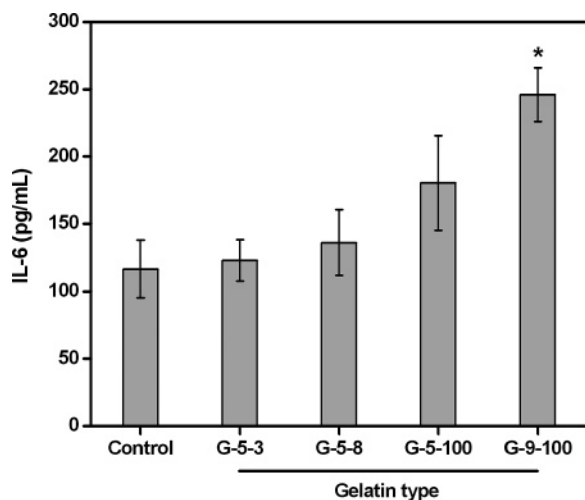


**Figure 7.** Level of IL-6 released from HCEC cultures after incubation for 2 days at 37 °C with various gelatin hydrogel disks. An asterisk indicates statistically significant differences ( $*p < 0.05$ ;  $n = 4$ ) as compared to controls (without materials).

received bioengineered cell sheets was significantly improved. However, intraocular grafting is different from the trials in corneal epithelial cell therapy because the unique physiological environments (i.e., anterior chamber and subretinal space) are perfused with large amounts of tissue fluid, which may cause unstable attachment of implanted cell sheets to lesion sites. In these cases, to deliver and retain the cells at the site of injury is an important factor in the design of related cell therapy

techniques. Therefore, it is necessary to provide a temporary support structure for enhancing the graft–host integration during tissue reconstruction. Compared with other reports on corneal endothelial cell transplantation using different carriers,<sup>4–7,19,20</sup> we have developed a novel method to deliver the cultivated HCEC monolayers by utilizing a biodegradable and cell-adhesive gelatin disk without permanent residence of carrier materials in vivo. On the basis of the aforementioned results, the gamma-sterilized hydrogel disks made from raw gelatins (IEP = 5.0, MW = 100 kDa) having stable mechanical properties, appropriate dissolution degree, and acceptable cytocompatibility were therefore selected in this study to carry the thermally detached HCEC sheets. After cell separation from thermoresponsive culture substrates at 20 °C, a bioadhesive gelatin disk was placed on the apical surface of the harvested HCEC sheets, and the gelatin-HCEC sheet constructs were spontaneously formed by a 5-min incubation at room temperature (Figure 8A). Given that HCECs in vivo possess polarity and pump water from corneal stroma into the anterior chamber, a proper orientation (i.e., apical side facing the aqueous humor) of the implanted HCECs must be maintained. After surgical insertion of the gelatin-HCEC sheet constructs into the rabbit anterior chamber, slit-lamp biomicroscopy revealed that the intact HCEC monolayers were positioned with uniform and correct polarity on the recipient corneas denuded of endothelial cells (Figure 8B). Because the swelling of gelatin carriers began immediately after exposure to the aqueous humor, the attached HCEC sheet grafts were further spread over the corneal posterior surface at 6 h postoperative (Figure 8C). The gelatin hydrogel

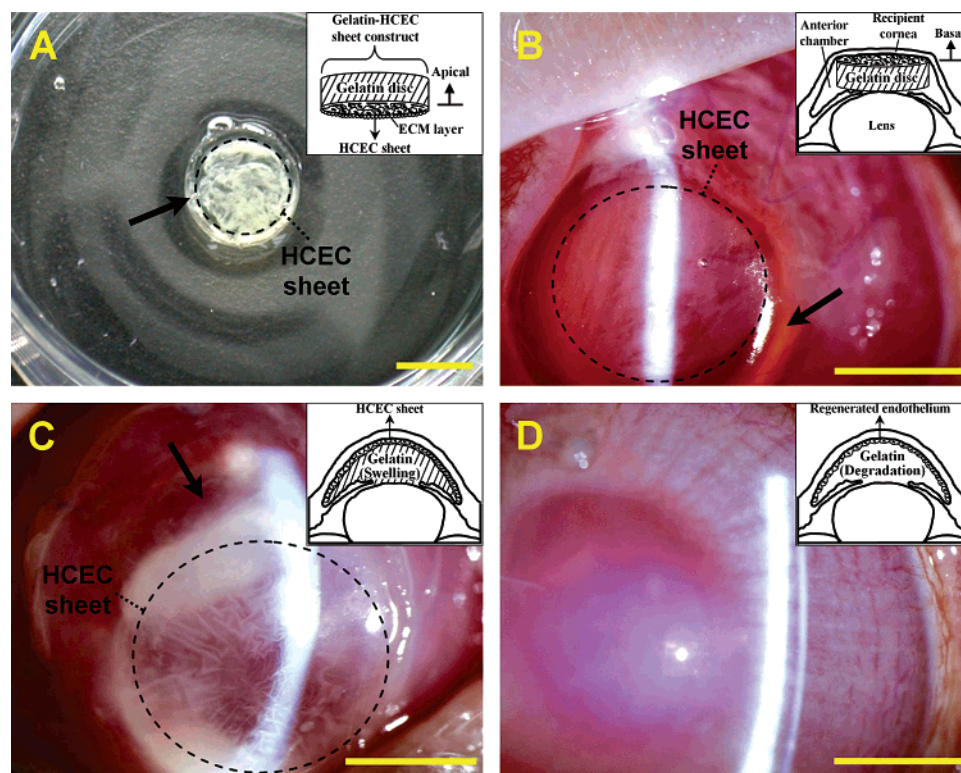


**Figure 8.** Gelatin carriers for intraocular delivery of thermally detached HCEC sheets. (A) After cell release from PNIPAAm-grafted culture surfaces at 20 °C, the gelatin-HCEC sheet constructs were made by using the 7-mm diameter gelatin disks (arrow) as a transparent and bioadhesive supporter for HCEC sheets with a size of around 0.75 cm<sup>2</sup>. (B) Under slit-lamp biomicroscopy, the rabbit anterior chamber was filled up with the rigid gelatin hydrogel carriers (arrow) after implantation of the gelatin-HCEC sheet constructs. The intact, round-shaped layer of HCECs was positioned onto the denuded corneal posterior surface. (C) At 6 h postoperative, the swelling of gelatin hydrogels (arrow) allowed the attachment and spread of HCEC sheet grafts on the lesion area of rabbit cornea, which may enhance subsequent graft–host integration. (D) At 6 weeks after cell sheet transplantation, the biodegradable gelatin carriers were disappeared in the anterior chamber, with the reconstructed corneal endothelium and returned corneal clarity. The insets showed the gelatin hydrogel carriers were used for intraocular delivery of cultivated HCEC sheets at each corresponding stage. Scale bars: 5 mm.



disks have largely degraded in vivo 6 weeks after surgery (Figure 8D). Additionally, the corneas have returned to a nearly normal thickness indicating the regeneration of corneal endothelium (Figure 8D). When endothelium alone was removed, the rabbit corneas became cloudy and remained opaque throughout the course of the experiment (data not shown). These results suggested that the corneal edema was reduced because of the function of implanted HCEC sheets. The advantage of our method for such an application is that it allows the cultivated HCEC sheets with their deposited extracellular matrix to be directly transplanted onto the damaged corneas without barriers caused by the use of cell carriers. Accompanied with the swelling and biodegradation of gelatin hydrogel disks, these well-organized HCEC sheet grafts are capable of integration into the host tissues. Since the foreign supporting materials are substantially completely absorbed in vivo, we believe that this novel cell therapy technique will have a high success rate in treating corneal endothelial cell loss.

### Conclusions

The development of grafting technology for thermally detached cell sheets is an important issue in regenerative medicine. Although biocompatible macromolecules seem to be well tolerated during short-term clinical use, the retention of foreign materials at lesion site may possibly cause corneal conditions, and thus the removal of supporting carriers is recommended after intraocular surgery. There is an increasing interest in biodegradable and bioabsorbable materials with specific biological functionality. In this report, by using a biodegradable and cell-adhesive gelatin hydrogel carrier, we established a novel methodology for the delivery of bioengineered HCEC sheets to corneal posterior surface from a thermoresponsive culture substrate. The functionality of gamma-sterilized cell carriers made from raw gelatins with different IEPs and MWs was investigated by the determination of mechanical properties, water content, and dissolution degree. In addition, the in vitro cytocompatibility studies allowed for the characterization of several key cellular responses, including cell proliferation, cell viability, and pro-inflammatory cytokine production to these hydrogel disks. These data provide an understanding of the optimal formulation of gelatin carrier preparation. For intraocular delivery of the cultured cell sheets, the use of gelatin carriers is very attractive because of the highly transparent and deformable nature of this hydrogel material. It is known that surgery with smaller incisions may provide faster rehabilitation and reduce postoperative morbidity. Currently, full-thickness corneal transplantation (penetrating keratoplasty, PK) is the common way to treat corneas that are opacified due to endothelial dysfunction. When compared with PK, the cell therapy techniques proposed in the present study enable intraocular grafting of HCEC sheets to be performed to occur with minimal surgical incisions. Therefore, the gamma-sterilized hydrogel disks made from raw gelatins (IEP = 5.0, MW = 100 kDa) are promising candidates as cell sheet carriers for effective corneal endothelial cell transplantation and therapy.

**Acknowledgment.** This work was supported financially by Grant NSC91-2320-B-007-007 from the National Science Council of Republic of China, by Grant VGHUST93-P6-25 from the Veterans General Hospitals University System of Taiwan Joint Research Program, and Grant NHRI94A1-MEAP01-001 from National Health Research Institutes.

### References and Notes

- Pan, Y. V.; Wesley, R. A.; Luginbuhl, R.; Denton, D. D.; Ratner, B. D. *Biomacromolecules* **2001**, *2*, 32–36.
- Schmaljohann, D.; Oswald, J.; Jørgensen, B.; Nitschke, M.; Beyerlein, D.; Werner, C. *Biomacromolecules* **2003**, *4*, 1733–1739.
- Ebara, M.; Yamato, M.; Aoyagi, T.; Kikuchi, A.; Sakai, K.; Okano, T. *Biomacromolecules* **2004**, *5*, 505–510.
- Jumblatt, M. M.; Maurice, D. M.; Schwartz, B. D. *Transplantation* **1980**, *29*, 498–499.
- Insler, M. S.; Lopez, J. G. *Curr. Eye Res.* **1990**, *9*, 23–30.
- Mohay, J.; Lange, T. M.; Soltan, J. B.; Wood, T. O.; McLaughlin, B. J. *Cornea* **1994**, *13*, 173–182.
- Mimura, T.; Yamagami, S.; Yokoo, S.; Usui, T.; Tanaka, K.; Hattori, S.; Irie, S.; Miyata, K.; Araie, M.; Amano, S. *Invest. Ophthalmol. Vis. Sci.* **2004**, *45*, 2992–2997.
- Demetriou, A. A.; Whiting, J. F.; Feldman, D.; Levenson, S. M.; Chowdhury, N. R.; Moscioni, A. D.; Kram, M.; Chowdhury, J. R. *Science* **1986**, *233*, 1190–1192.
- Lu, L.; Yaszemski, M. J.; Mikos, A. G. *Biomaterials* **2001**, *22*, 3345–3355.
- Yamato, M.; Okano, T. *Mater. Today* **2004**, *7*, 42–47.
- Yang, J.; Yamato, M.; Kohno, C.; Nishimoto, A.; Sekine, H.; Fukai, F.; Okano, T. *Biomaterials* **2005**, *26*, 6415–6422.
- Hirose, M.; Kwon, O. H.; Yamato, M.; Kikuchi, A.; Okano, T. *Biomacromolecules* **2000**, *1*, 377–381.
- Shimizu, T.; Yamato, M.; Akutsu, T.; Shibata, T.; Isoi, Y.; Kikuchi, A.; Umezumi, M.; Okano, T. *J. Biomed. Mater. Res.* **2002**, *60*, 110–117.
- Nishida, K.; Yamato, M.; Hayashida, Y.; Watanabe, K.; Maeda, N.; Watanabe, H.; Yamamoto, K.; Nagai, S.; Kikuchi, A.; Tano, Y.; Okano, T. *Transplantation* **2004**, *77*, 379–385.
- Shimizu, T.; Yamato, M.; Isoi, Y.; Akutsu, T.; Setomaru, T.; Abe, K.; Kikuchi, A.; Umezumi, M.; Okano, T. *Circ. Res.* **2002**, *90*, e40–e48.
- Nishida, K.; Yamato, M.; Hayashida, Y.; Watanabe, K.; Yamamoto, K.; Adachi, E.; Nagai, S.; Kikuchi, A.; Maeda, N.; Watanabe, H.; Okano, T.; Tano, Y. *New Engl. J. Med.* **2004**, *351*, 1187–1196.
- Shiroyanagi, Y.; Yamato, M.; Yamazaki, Y.; Toma, H.; Okano, T. *BJU Int.* **2004**, *93*, 1069–1075.
- Akizuki, T.; Oda, S.; Komaki, M.; Tsuchioka, H.; Kawakatsu, N.; Kikuchi, A.; Yamato, M.; Okano, T.; Ishikawa, I. *J. Periodont. Res.* **2005**, *40*, 245–251.
- Lange, T. M.; Wood, T. O.; McLaughlin, B. J. *J. Cataract Refract. Surg.* **1993**, *19*, 232–235.
- Ishino, Y.; Sano, Y.; Nakamura, T.; Connon, C. J.; Rigby, H.; Fullwood, N. J.; Kinoshita, S. *Invest. Ophthalmol. Vis. Sci.* **2004**, *45*, 800–806.
- McCulley, J. P.; Maurice, D. M.; Schwartz, B. D. *Ophthalmology* **1980**, *87*, 194–201.
- Hsiue, G. H.; Lai, J. Y.; Chen, K. H.; Hsu, W. M. *Transplantation* **2006**, *81*, 473–476.
- Chiellini, E.; Cinelli, P.; Grillo Fernandes, E.; Kenawy, E. R. S.; Lazzeri, A. *Biomacromolecules* **2001**, *2*, 806–811.
- Okamoto, T.; Yamamoto, Y.; Gotoh, M.; Huang, C. L.; Nakamura, T.; Shimizu, Y.; Tabata, Y.; Yokomise, H. *J. Thorac. Cardiovasc. Surg.* **2004**, *127*, 329–334.
- Hokugo, A.; Ozeki, M.; Kawakami, O.; Sugimoto, K.; Mushimoto, K.; Morita, S.; Tabata, Y. *Tissue Eng.* **2005**, *11*, 1224–1233.
- Tabata, Y.; Ikada, Y. *Adv. Drug Delivery Rev.* **1998**, *31*, 287–301.
- Morimoto, K.; Chono, S.; Kosai, T.; Seki, T.; Tabata, Y. *J. Pharm. Pharmacol.* **2005**, *57*, 839–844.
- Fukunaka, Y.; Iwanaga, K.; Morimoto, K.; Kakemi, M.; Tabata, Y. *J. Controlled Release* **2002**, *80*, 333–343.
- Kushibiki, T.; Matsumoto, K.; Nakamura, T.; Tabata, Y. *Gene Ther.* **2004**, *11*, 1205–1214.
- Hsiue, G. H.; Lai, J. Y.; Lin, P. K. *J. Biomed. Mater. Res.* **2002**, *61*, 19–25.
- Park, H.; Temenoff, J. S.; Holland, T. A.; Tabata, Y.; Mikos, A. G. *Biomaterials* **2005**, *26*, 7095–7103.
- Miyoshi, M.; Kawazoe, T.; Igawa, H. H.; Tabata, Y.; Ikada, Y.; Suzuki, S. *J. Biomater. Sci.-Polym. Ed.* **2005**, *16*, 893–907.
- Taira, M.; Furuuchi, H.; Saitoh, S.; Sugiyama, Y.; Sekiyama, S.; Araki, Y.; Tabata, Y. *J. Oral Rehabil.* **2005**, *32*, 382–387.
- Zekorn, D. *Bibl. Haematol.* **1969**, *33*, 131–140.
- Guidoin, R.; Marceau, D.; Rao, T. J.; King, M.; Merhi, Y.; Roy, P. E.; Martin, L.; Duval, M. *Biomaterials* **1987**, *8*, 433–441.
- Otani, Y.; Tabata, Y.; Ikada, Y. *Biomaterials* **1998**, *19*, 2091–2098.



- (37) Tabata, Y.; Uno, K.; Yamaoka, T.; Ikada, Y.; Muramatsu, S. *Cancer Res.* **1991**, *51*, 5532–5538.
- (38) Kushibiki, T.; Matsuoka, H.; Tabata, Y. *Biomacromolecules* **2004**, *5*, 202–208.
- (39) Choksakulnimitr, S.; Masuda, S.; Tokuda, H.; Takakura, Y.; Hashida, M. *J. Controlled Release* **1995**, *34*, 233–241.
- (40) Chen, K. H.; Azar, D.; Joyce, N. C. *Cornea* **2001**, *20*, 731–737.
- (41) Chen, K. H.; Hsu, W. M.; Chiang, C. C.; Li, Y. S. *Curr. Eye Res.* **2003**, *26*, 363–370.
- (42) Harris, D. L.; Joyce, N. C. *J. Interferon Cytokine Res.* **1999**, *19*, 327–334.
- (43) Fischbach, C.; Tessmar, J.; Lucke, A.; Schnell, E.; Schmeer, G.; Blunk, T.; Göpferich, A. *Surf. Sci.* **2001**, *491*, 333–345.
- (44) Bigi, A.; Panzavolta, S.; Rubini, K. *Biomaterials* **2004**, *25*, 5675–5680.
- (45) Katz, E. P.; Li, S. T. *J. Mol. Biol.* **1973**, *73*, 351–369.
- (46) Trudel, J.; Massia, S. P. *Biomaterials* **2002**, *23*, 3299–3307.
- (47) Carlson, K. H.; Bourne, W. M.; Brubaker, R. F. *Invest. Ophthalmol. Vis. Sci.* **1988**, *29*, 185–193.
- (48) Malchiodi-Albedi, F.; Morgillo, A.; Formisano, G.; Paradisi, S.; Perilli, R.; Scalzo, G. C.; Scordia, G.; Caiazza, S. *J. Biomed. Mater. Res.* **2002**, *60*, 548–555.
- (49) Sobottka Ventura, A. C.; Böhnke, M. *Br. J. Ophthalmol.* **2001**, *85*, 1110–1114.

BM0601575